Available online at www.sciencedirect.com
ScienceDirect
Ceramics International 37 (2011) 2215–2220
CERAMICS INTERNATIONAL
www.elsevier.com/locate/ceramint

Electrochemical properties of $LiCo_yMn_{2-y}O_4$ synthesized using a combustion method in a voltage range of 3.5–5.0 V

Myoung Youp Song [a,*], Ik Hyun Kwon [b], Hye Ryoung Park [c], Daniel R. Mumm [d]

[a] Division of Advanced Materials Engineering, Department of Hydrogen and Fuel Cells, Hydrogen & Fuel Cell Research Center, Engineering Research Institute, Chonbuk National University, 664-14 1ga Deogjindong Deogjingu, Jeonju 561-756, Republic of Korea
[b] Jeonbuk Technopark Regional Industry Evaluation Agency 723-1, 2ga Palbok-Dong, Dukjin-gu, Jeonju, Jeonbuk 561-844, Republic of Korea
[c] School of Applied Chemical Engineering, Chonnam National University, 300 Yongbongdong Bukgu, Gwangju 500-757, Republic of Korea
[d] Department of Chemical Engineering and Materials Science, University of California, Irvine, CA 92697-2575, USA

Received 20 October 2010; received in revised form 31 January 2011; accepted 7 March 2011
Available online 14 April 2011

Abstract

$LiCo_yMn_{2-y}O_4$ ($y = 0.00$, 0.04 and 0.08) were synthesized using a combustion method, and the electrochemical properties were examined in the voltage range of 3.5–5.0 V. The XRD patterns of the synthesized samples were similar, and the samples had a spinel phase structure. The first charge capacity curves exhibited an inflection in the voltage range of 4.2–5.0 V, where it is believed that additional, previously unreported phase transition occurs. The voltage vs. x curves for the first to fifth cycle exhibited two distinct voltage plateaus, corresponding well to a two-phase reaction and a one-phase reaction, respectively, as reported previously. For the voltage range of 3.5–5.0 V, the first discharge capacity increased and the cycling performance improved as y increased. Among these samples, $LiCo_{0.08}Mn_{1.92}O_4$ had the largest first discharge capacity of 132.5 mA h/g at 600 $\mu A/cm^2$, and its cycling efficiency was 91.1% at the 15th cycle in the voltage range of 3.5–5.0 V.

Keywords: $LiCo_yMn_{2-y}O_4$; Combustion method; First discharge capacity; Cycling performance; Plateaus

1. Introduction

Transition metal oxides such as $LiCoO_2$ [1–3], $LiNiO_2$ [4,5] and $LiMn_2O_4$ [6–12] have been investigated for their use as cathode materials in lithium secondary batteries. $LiCoO_2$ has a large diffusivity and a high operating voltage, and can be easily prepared. Nevertheless, it contains an expensive element, Co. $LiNiO_2$ has a large discharge capacity [13] and is relatively excellent from the view points of economics and environment. However, its preparation is very difficult compared with those of $LiCoO_2$ and $LiMn_2O_4$. $LiMn_2O_4$ does not have a good cycling performance, but it is very cheap and does not bring about environmental pollution.

$LiMn_2O_4$ is usually synthesized through a solid-state reaction method which uses mechanical mixing followed by high-temperature sintering. $LiMn_2O_4$ compounds are made from stoichiometric amounts of Li salts such as LiOH, $LiNO_3$, and Li_2CO_3, mixed with manganese oxides [chemical manganese dioxides (CMD) or electrochemical manganese dioxides (EMD)] [14–19].

The solid-state reaction method has numerous disadvantages: difficulty in a homogeneous formation of phase, formation of particles with non-uniform size and shape, and difficulty in the formation of a compound with stoichiometric composition. On the other hand, the homogeneous mixing of the starting materials can be accomplished using the combustion method because in this method nitrates as starting materials and urea as a fuel are mixed in distilled water by a magnetic stirrer. This may lead to good crystallinity and a homogeneous particle size when the sample is synthesized.

Liu et al. [20] reported that partial substitution of a small quantity of Co for the Mn can significantly improve the cycling behavior of $LiMn_2O_4$. Shen et al. [21] reported that chemical substitution of Co^{+3} for Mn^{+3} in $LiMn_2O_4$ improved the cathodic properties and the efficiency in maintaining electrochemical capacity over a large number of cycles without sacrificing the initial reversible capacity and performance at temperature below room temperature.

* Corresponding author. Tel.: +82 63 270 2379; fax: +82 63 270 2386.
E-mail address: songmy@jbnu.ac.kr (M.Y. Song).

0272-8842/$36.00
doi:10.1016/j.ceramint.2011.03.071

In this work, we chose Co as a substituting element for Mn in $LiMn_2O_4$ to improve the electrochemical properties of $LiMn_2O_4$. We synthesized $LiCo_yMn_{2-y}O_4$ ($y = 0.00$, 0.04 and 0.08) via the combustion method using nitrates and urea as starting materials and examined their electrochemical properties in a voltage range of 3.5–5.0 V. The upper limit of the voltage range, 5.0 V, is quite a higher voltage than that usually used in research on the electrochemical properties of $LiMn_2O_4$.

2. Experimental

$LiCo_yMn_{2-y}O_4$ ($y = 0.00$, 0.04 and 0.08) were synthesized using a combustion method. Starting materials were $LiNO_3$, $Mn(NO_3)_2{\cdot}6H_2O$, $Co(NO_3)_2{\cdot}6H_2O$, and NH_2CONH_2 (urea) with purities of 98%. The starting materials in the desired compositions were mixed homogeneously by a magnetic stirrer. The mixed samples were in light reddish brown color. These mixed samples were preheated at 400 °C for 4 h, and then calcined two times at 750 °C for 24 h. The heating rate was 100 °C/h and the cooling rate was 50 °C/h. Phase identification of the prepared samples was carried out via X-ray diffraction (XRD, Rigaku III/A type) analysis using Cu Kα radiation. The morphologies of the samples were observed using a scanning electron microscope (SEM). To measure the electrochemical properties, the electrochemical cells consisted of the prepared sample as a positive electrode, Li metal as a negative electrode, and an electrolyte of 1 M $LiPF_6$ in a volumetric 1:1 ratio mixture of ethylene carbonate (EC) and dimethyl carbonate (DMC). A Whatman glass was used as a separator. The cells were assembled in an argon-filled dry box. To fabricate the positive electrode, active material, acetylene black and polytetrafluoroethylene (PTFE) binder were mixed in a 100:10:1 weight ratio in an agate mortar. By introducing the Li metal, the Whatman glass-fiber, the positive electrode and the electrolyte, the cell was assembled. All electrochemical tests were performed at room temperature with a battery charge–discharge cycle tester (WonATec WBCS 3000) at a current density of 600 μA/cm^2 in a voltage range from 3.5 to 5.0 V.

3. Results and discussion

The XRD patterns of $LiCo_yMn_{2-y}O_4$ ($y = 0.00$, 0.04 and 0.08) synthesized via the combustion method were obtained. They were similar, but the diffraction angles increased as y increased, indicating that the lattice parameter decreased as y increased. Samples were identified as being in the spinel phase with a space group of $Fd\overline{3}m$. The lattice parameters of these samples were larger than that of $LiMn_2O_4$ synthesized using the solid-state method [22].

The SEM photographs of $LiMn_2O_4$ calcined for 24 h and $LiCo_yMn_{2-y}O_4$ ($y = 0.00$, 0.04 and 0.08) calcined for 48 h are presented in Fig. 1. The particles of $LiMn_2O_4$ calcined for 48 h are larger than those of the $LiMn_2O_4$ calcined for 24 h. Particles for $y = 0.00$ calcined for 48 h are larger than those for $y = 0.04$ and 0.08 calcined for 48 h. The particles for $y = 0.04$ and 0.08 are fine and homogeneous with a spherical shape and are similar in shape; however, particles for $y = 0.04$ were slightly finer than those for $y = 0.08$.

Fig. 2 shows the variations in voltage vs. discharge capacity curve with the number of cycles, n, for $LiCo_yMn_{2-y}O_4$

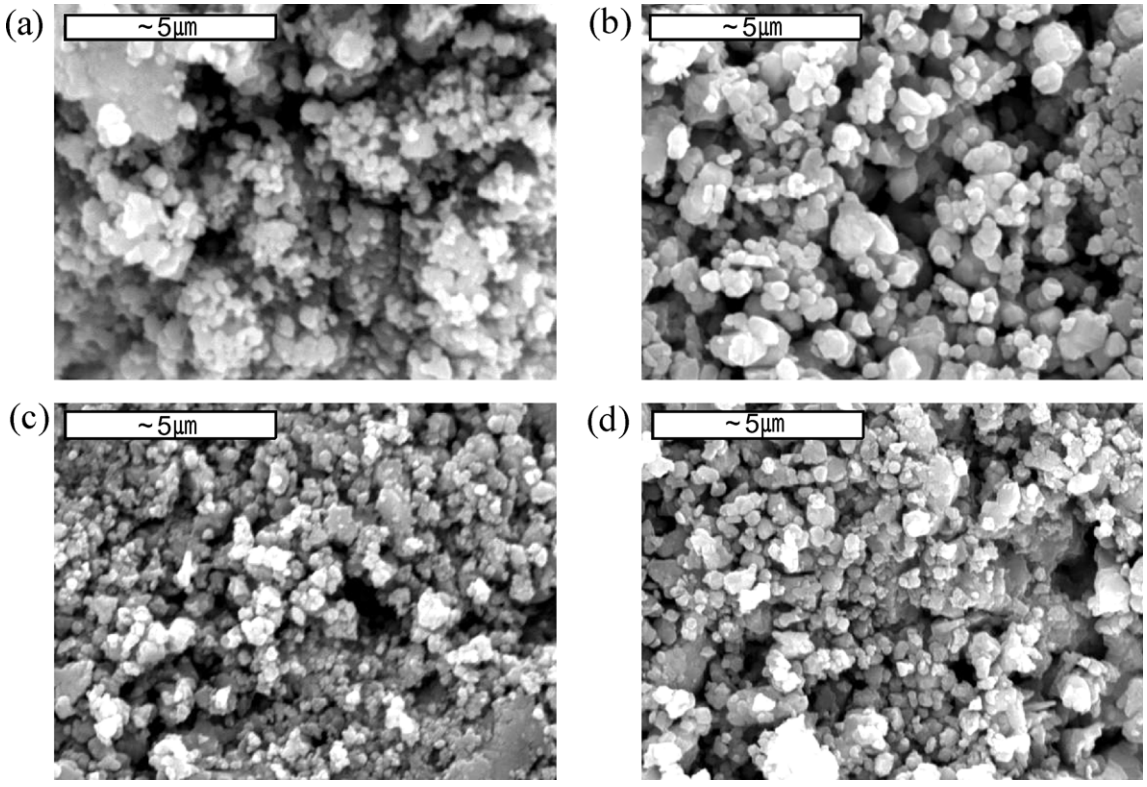

Fig. 1. SEM photographs of $LiCo_yMn_{2-y}O_4$ [(a) $y = 0.00$/24 h; (b) $y = 0.00$/48 h; (c) $y = 0.04$/48 h; and (d) $y = 0.08$/48 h] synthesized via the combustion method.

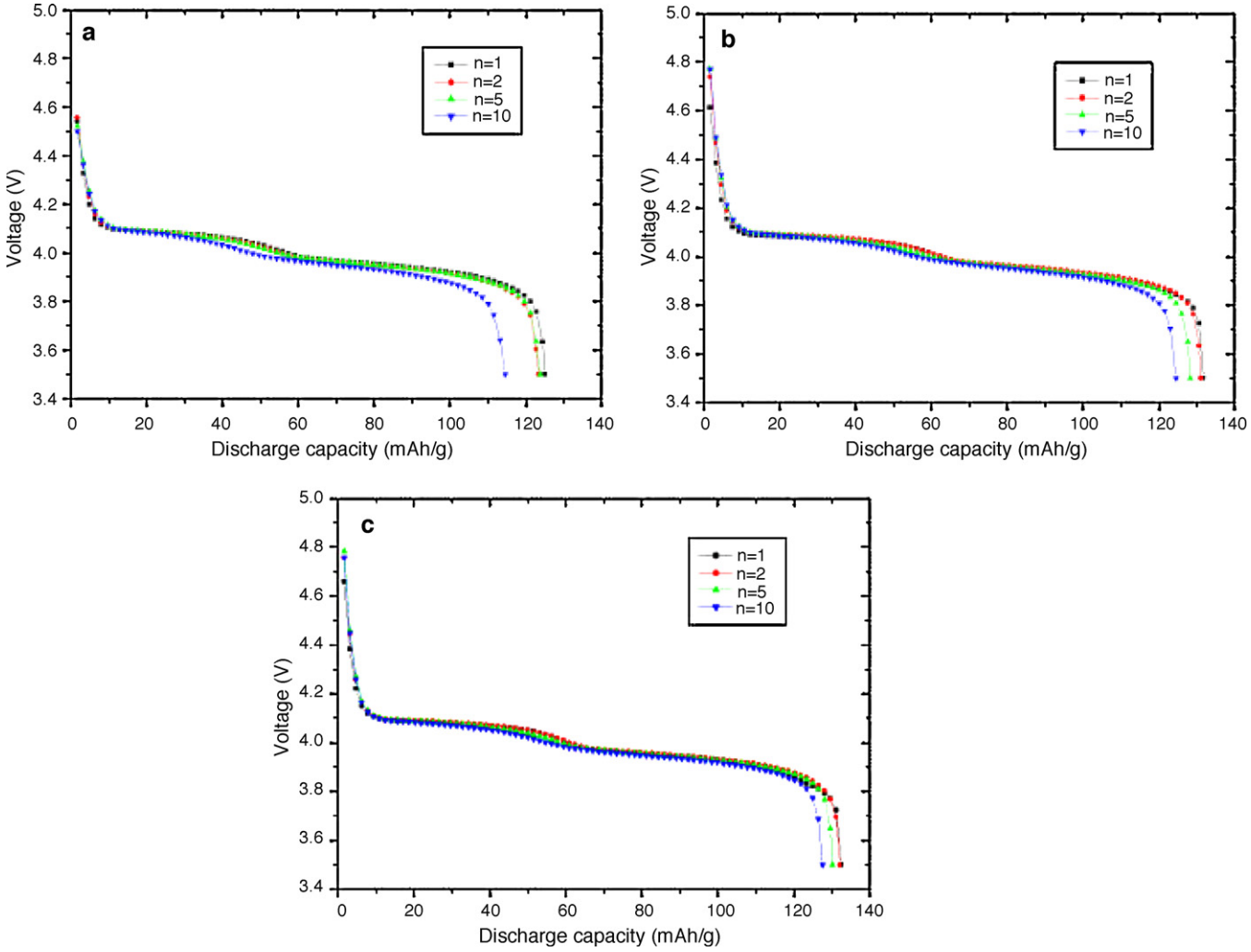

Fig. 2. Variations in voltage vs. discharge capacity curve with the number of cycles for $LiCo_yMn_{2-y}O_4$ synthesized using the combustion method in the voltage range of 3.5–5.0 V at 600 μA/cm^2; (a) $y = 0.00$, (b) $y = 0.04$, and (c) $y = 0.08$.

($y = 0.00$, 0.04 and 0.08) synthesized using the combustion method. For these curves, the voltage range is 3.5–5.0 V, and the current density is 600 μA/cm^2. All of the curves exhibit two voltage plateaus, corresponding to a two-phase reaction and a one-phase reaction, respectively. The voltages of the two plateaus are 4.06 and 3.92 V for $y = 0.00$, 4.07 and 3.94 V for $y = 0.04$, and 4.08 and 3.95 V for $y = 0.08$. The voltages of the two voltage plateaus are similar to those reported by Yoshio for $LiMn_2O_4$ [23], i.e., 4.10 and 4.05 V. As y increases, the rate of decrease in the discharge capacity with the number of cycles becomes lower. As the number of cycles increases, the length of the higher plateau decreases. As y increases, the rate of decrease in the length of the higher plateau diminishes.

The voltage vs. the first charge capacity curves for $LiCo_yMn_{2-y}O_4$ ($y = 0.00$, 0.04 and 0.08) synthesized using the combustion method in the voltage range of 3.5–5.0 V at 600 μA/cm^2 are shown in Fig. 3. Enlarged curves are also given. All curves exhibit an inflection in the voltage range of 4.2–5.0 V, where it is believed that additional, previously unreported phase transition occurs.

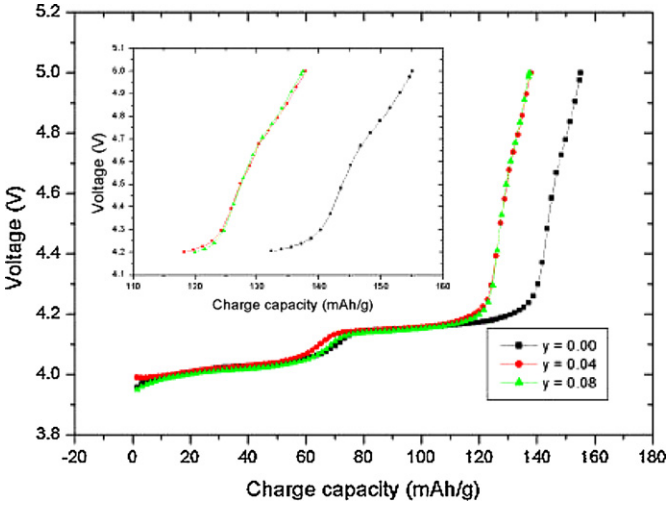

Fig. 3. Voltage vs. the first charge capacity curves for $LiCo_yMn_{2-y}O_4$ ($y = 0.00$, 0.04 and 0.08) synthesized using the combustion method in the voltage range of 3.5–5.0 V at 600 μA/cm^2.

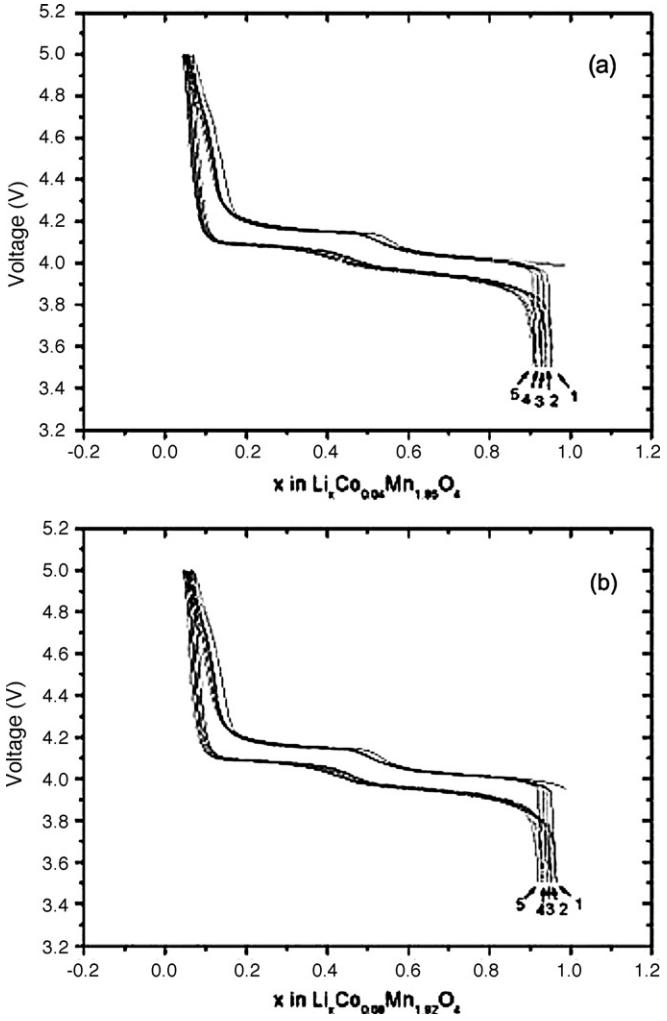

Fig. 4. Voltage vs. x curves of $LiCo_yMn_{2-y}O_4$ synthesized using the combustion method for the first to fifth cycle in the voltage range of 3.5–5.0 V at 600 μA/cm^2; (a) $y = 0.04$ and (b) $y = 0.08$.

Fig. 4 presents voltage vs. x curves of $LiCo_yMn_{2-y}O_4$ ($y = 0.04$ and 0.08) synthesized using the combustion method for the first to fifth cycle. For these curves, the voltage range is 3.5–5.0 V and the current density is 600 μA/cm^2. All of the curves exhibit two distinct voltage plateaus, corresponding well to the results by Xia and Yoshio [14]. They reported that a two-phase reaction (cubic $a_0 = 8.154$ Å and $a_0 = 8.072$ Å) occurred in the range $0.1 < x < 0.45$, and a one-phase reaction (cubic $a_0 = 8.163$–8.247 Å) occurred in the range $0.45 < x < 1.0$ for the first charge.

The variations in the discharge capacity at 600 μA/cm^2 with the number of cycles for $LiCo_yMn_{2-y}O_4$ ($y = 0.00$, 0.04 and 0.08) synthesized using the combustion method are provided in Fig. 5. For these curves, the voltage range is 3.5–5.0 V. The sample for $y = 0.00$ has the smallest first discharge capacity (125.0 mA h/g), and as y increases, the first discharge capacity increases. $LiCo_{0.08}Mn_{1.92}O_4$ has the largest first discharge capacity of 132.5 mA h/g and $LiCo_{0.04}Mn_{1.96}O_4$ has the first discharge capacity of 131.6 mA h/g. $LiCo_{0.08}Mn_{1.92}O_4$ has the largest discharge capacities from $n = 1$ to $n = 15$, followed in

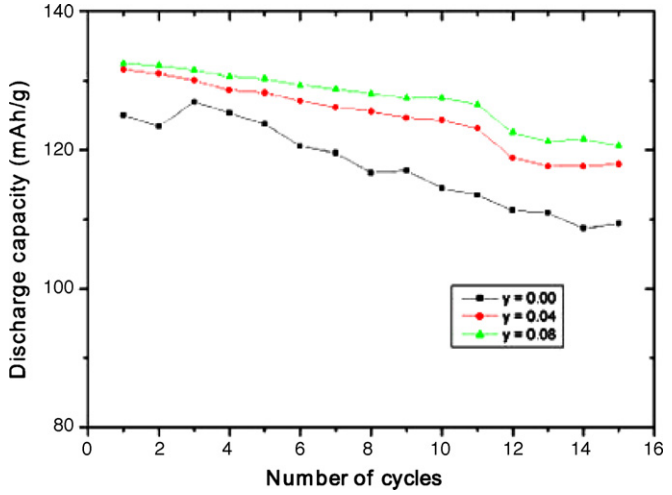

Fig. 5. Variations in the discharge capacity at 600 μA/cm^2 with the number of cycles for $LiCo_yMn_{2-y}O_4$ ($y = 0.00$, 0.04 and 0.08) synthesized using the combustion method in the voltage range of 3.5–5.0 V.

order by $LiCo_{0.04}Mn_{1.96}O_4$ and $LiMn_2O_4$. That is, as y increases, the discharge capacities increase, contrary to the results reported previously. In addition, the cycling performance improves as y increases. The cycling efficiencies (the discharge capacity divided by the first discharge capacity) at the 15th cycle were 87.6% for $LiMn_2O_4$, 89.6% for $LiCo_{0.04}Mn_{1.96}O_4$, and 91.1% for $LiCo_{0.08}Mn_{1.92}O_4$.

Fig. 6 shows the variations in the discharge capacity at 600 μA/cm^2 with the number of cycles for $LiCo_yMn_{2-y}O_4$ ($y = 0.00$, 0.04 and 0.08) synthesized using the combustion method and for $LiMn_2O_4$ synthesized using the solid-state method. For these curves, the voltage range is 3.5–4.3 V. The sample for $y = 0.00$ synthesized using the combustion method has the largest first discharge capacity (125.3 mA h/g), and as y increases, the first discharge capacity decreases. However, the cycling performance improves as y increases. The sample with

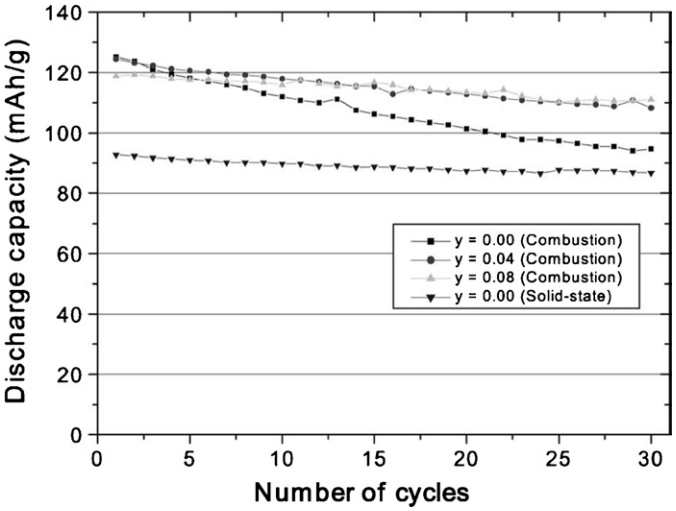

Fig. 6. Variations in the discharge capacity with the number of cycles for $LiCo_yMn_{2-y}O_4$ ($y = 0.00$, 0.04 and 0.08) synthesized using the combustion method and for $LiMn_2O_4$ synthesized using the solid-state method, in the voltage range of 3.5–4.3 V at 600 μA/cm^2.

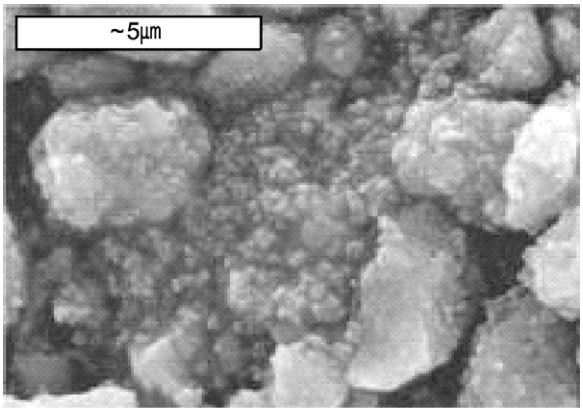

Fig. 7. SEM photograph of $LiMn_2O_4$ synthesized using the solid-state reaction method.

$y = 0.08$ has the first discharge capacity of 118.8 mA h/g and a discharge capacity of 111.0 mA h/g at the 13th cycle. The improvement in cycling performance with the increase in y agrees well with the previously reported results. Many works [24–27] reported that partial substitution of small quantities of metal cations for the Mn can significantly improve the cycling behavior of $LiMn_2O_4$. $LiMn_2O_4$ synthesized using the solid-state reaction method has a good cycling performance, but the first discharge capacity (92.8 mA h/g) is smaller than those for the samples synthesized using the combustion method.

The SEM photograph of $LiMn_2O_4$ synthesized using the solid-state reaction method is shown in Fig. 7. The sample exhibits an inhomogeneous distribution of small particles, and large particles having small particles on their surface. $LiMn_2O_4$ was synthesized from starting materials, $LiOH{\cdot}H_2O$, MnO_2, and $CoCO_3$ with purities of 99%. The mixed starting materials in desired compositions were preheated at 400 °C for 10 h, and then calcined two times at 750 °C for 24 h after grinding, mixing, and pelletizing. The heating rate was 100 °C/h and the cooling rate was 50 °C/h.

As mentioned above, the variation in the lattice parameter with y in $LiCo_yMn_{2-y}O_4$ synthesized using the combustion method was investigated, and that for $LiMn_2O_4$ synthesized using the solid-state method was also obtained [22]. The lattice parameter decreased as y increased. The lattice parameters of the samples using the combustion method were larger than that of $LiMn_2O_4$ synthesized using the solid-state method.

For the voltage range of 3.5–4.3 V, the first discharge capacity decreased and the cycling performance improved as y increased. On the other hand, for the voltage range of 3.5–5.0 V, the first discharge capacity increased and the cycling performance improved as y increased. $LiCo_{0.08}Mn_{1.92}O_4$ had the largest first discharge capacity of 132.5 mA h/g, and its cycling efficiency was 91.1% at the 15th cycle for the voltage range of 3.5–5.0 V.

For the voltage range of 3.5–4.3 V at 600 μA/cm^2, $LiMn_2O_4$ synthesized using the combustion method had the first discharge capacity of 125.3 mA h/g, while that synthesized using the solid-state reaction had the first discharge capacity of 92.8 mA h/g. For the voltage range of 3.5–5.0 V at 600 μA/cm^2, $LiMn_2O_4$ synthesized using the combustion method had the first discharge capacity of 125.0 mA h/g. The SEM photograph for $LiMn_2O_4$ synthesized using the solid-state method showed an inhomogeneous distribution of large particles and small particles. The superior crystallinity, the larger lattice parameter, and the finer and more homogeneous particles of $LiMn_2O_4$ synthesized via the combustion method, compared with those for $LiMn_2O_4$ synthesized via the solid-state method, are considered to lead to the larger discharge capacity of $LiMn_2O_4$.

4. Conclusions

$LiCo_yMn_{2-y}O_4$ ($y = 0.00$, 0.04 and 0.08) were synthesized using the combustion method by preheating at 400 °C for 4 h and then calcining two times at 750 °C for 24 h. The XRD patterns of $LiCo_yMn_{2-y}O_4$ ($y = 0.00$, 0.04 and 0.08) synthesized via the combustion method were similar, and the samples had a spinel phase structure. The first charge capacity curves exhibited an inflection in the voltage range of 4.2–5.0 V, where it is believed that additional, previously unreported phase transition occurs. For the voltage range of 3.5–5.0 V, the first discharge capacity increased and the cycling performance improved as y increased. Among the $LiCo_yMn_{2-y}O_4$ ($y = 0.00$, 0.04 and 0.08) samples, $LiCo_{0.08}Mn_{1.92}O_4$ had the largest first discharge capacity of 132.5 mA h/g at 600 μA/cm^2, and its cycling efficiency was 91.1% at the 15th cycle in the voltage range of 3.5–5.0 V. The superior crystallinity, the larger lattice parameter, and the finer and more homogeneous particles of $LiMn_2O_4$ synthesized via the combustion method, compared with those for $LiMn_2O_4$ synthesized via the solid-state method, are considered to lead to the larger discharge capacity of $LiMn_2O_4$.

References

[1] K. Ozawa, Solid State Ionics 69 (1994) 212.
[2] R. Alcantara, P. Lavela, J.L. Tirado, R. Stoyanova, E. Zhecheva, J. Solid State Chem. 134 (1997) 265.
[3] Z.S. Peng, C.R. Wan, C.Y. Jiang, J. Power Sources 72 (1998) 215.
[4] J.M. Tarascon, E. Wang, F.K. Shokoohi, W.R. McKinnon, S. Colson, J. Electrochem. Soc. 138 (1991) 2859.
[5] A.R. Armstrong, P.G. Bruce, Lett. Nat. 381 (1996) 499.
[6] J.R. Dahn, U. von Sacken, C.A. Michal, Solid State Ionics 44 (1990) 87.
[7] J.R. Dahn, U. von Sacken, M.W. Juzkow, H. Al-Janaby, J. Electrochem. Soc. 138 (1991) 2207.
[8] A. Marini, V. Massarotti, V. Berbenni, D. Capsoni, R. Riccardi, E. Antolini, B. Passalacqua, Solid State Ionics 45 (1991) 143.
[9] W. Ebner, D. Fouchard, L. Xie, Solid State Ionics 69 (1994) 238.
[10] M.Y. Song, D.S. Ahn, Solid State Ionics 112 (1998) 21.
[11] M.Y. Song, D.S. Ahn, H.R. Park, J. Power Sources 83 (1999) 57.
[12] D.S. Ahn, M.Y. Song, J. Electrochem. Soc. 147 (3) (2000) 874.
[13] Y. Nishida, K. Nakane, T. Stoh, J. Power Sources 68 (1997) 561.
[14] Y. Xia, M. Yoshio, J. Electrochem. Soc. 143 (1996) 825.
[15] A. Momchilov, V. Manev, A. Nassalevska, J. Power Sources 41 (1993) 305.
[16] G. Pistoia, G. Wang, J. Electrochem. Soc. 66 (1993) 135.
[17] J.M. Tarascon, W.R. McKinnon, F. Coowar, T.N. Bowmer, G. Amatucci, D. Guyomard, J. Electrochem. Soc. 141 (1994) 1421.
[18] Z. Jiang, K.M. Abraham, J. Electrochem. Soc. 143 (1996) 1591.
[19] G. Pistoia, D. Zane, Y. Zhang, J. Electrochem. Soc. 142 (1995) 2551.
[20] W. Liu, K. Kowal, G.C. Farrington, J. Electrochem. Soc. 143 (1996) 3590.

[21] C.H. Shen, R.S. Liu, R. Gundakaram, J.M. Chen, S.M. Huang, J.S. Chen, C.M. Wang, J. Power Sources 102 (2001) 21.
[22] I.H. Kwon, M.Y. Song, Solid State Ionics 158 (1–2) (2003) 103.
[23] M. Yoshio, Lithium Ion Batteries (General), Springer Publishing, 1996, p. 182.
[24] R.J. Gummow, A. de Kock, M.M. Thackeray, Solid State Ionics 69 (1994) 59.
[25] R. Bittihn, R. Herr, D.J. Hoge, Power Sources 43–44 (1993) 223.
[26] H. Guohua S Ikuta, T. Uchida, M. Wakihara, J. Electrochem. Soc. 143 (1996) 178.
[27] K. Amine, H. Tukamoto, H. Yasuda, Y. Fujita, J. Electrochem. Soc. 143 (1996) 1607.